Available online at www.sciencedirect.com
ScienceDirect
Ceramics International 37 (2011) 2311–2316
CERAMICS INTERNATIONAL
www.elsevier.com/locate/ceramint

Bioactive glass nanoparticles with negative zeta potential

Ali Doostmohammadi [a,b,*], Ahmad Monshi [a], Rasoul Salehi [c], Mohammad Hossein Fathi [a], Zahra Golniya [a], Alma. U. Daniels [d]

[a] Biomaterials Group, Materials Engineering Department, Isfahan University of Technology, Isfahan 84156-83111, Iran
[b] Isfahan University of Medical Sciences, Isfahan 81746-73461, Iran
[c] Department of Genetics and Molecular Biology, School of Medicine, Isfahan University of Medical Sciences, Isfahan 81746-73461, Iran
[d] Laboratory of Biomechanics & Biocalorimetry, Coalition for Clinical Morphology & Biomedical Engineering, University of Basel Faculty of Medicine, Basel, Switzerland

Received 3 March 2011; accepted 15 March 2011
Available online 23 March 2011

Abstract

The purpose of this work was to produce and characterize SiO_2–CaO–P_2O_5 bioactive glass nanoparticles with negative zeta potential for possible use in biomedical applications. 63S bioactive glass was obtained using the sol–gel method. X-ray fluorescence (XRF) spectroscopy and dispersive X-ray analysis (EDX) confirmed the preparation of the 63S bioactive glass with 62.17% SiO_2, 28.47% CaO and 9.25% P_2O_5 (in molar percentage). The in vitro apatite forming ability of prepared bioactive glass was evaluated by Fourier transform infrared spectroscopy (FTIR) after immersion in simulated body fluid (SBF). The result showed that high crystalline hydroxyapatite can form on glass particles. By the gas adsorption (BET method), particle specific surface area and theoretical particle size were 223.6 ± 0.5 m^2/g and ~24 nm, respectively. Laser dynamic light scattering (DLS) indicated particles were mostly agglomerated and had an average diameter between 100 and 500 nm. Finally, using laser Doppler electrophoresis (LDE) the zeta potential of bioactive glass nanoparticles suspended in physiological saline was determined. The zeta potential was negative for acidic, neutral and basic pH values and was -16.18 ± 1.8 mV at pH 7.4. In summary, the sol–gel derived nanoparticles revealed in vitro bioactivity in SBF and had a negative zeta potential in physiological saline solution. This negative surface charge is due to the amount and kind of the ions in glass structure and according to the literature, promotes cell attachment and facilitates osteogenesis. The nanometric particle size, bioactivity and negative zeta potential make this material a possible candidate for bone tissue engineering.
© 2011 Elsevier Ltd and Techna Group S.r.l. All rights reserved.

Keywords: A. Sol–gel processes; C. Chemical properties; D. Glass; E. Biomedical applications

1. Introduction

Bioactive glasses (SiO_2 glasses containing Ca and P) are well-known materials for use in implant applications, and have been shown to augment formation of bone and other tissues [1]. Bioactive glasses in the system SiO_2–CaO–P_2O_5 obtained by sol–gel method present good characteristics of osteoconduction and osteoinduction. They can be designed with controlled compositions and high specific surface area in order to be biodegradable [2,3]. Compared to particle of μm or larger sizes, bioactive glass nanoparticles may provide a means for more rapid release of Ca and P where this is desired [4].

Additionally, recent findings have demonstrated that there is a genetic control of the cellular response to bioactive glass materials [5–7]. Seven families of genes are up-regulated when primary human osteoblasts are exposed to the ionic dissolution products of bioactive glasses [7]. These findings indicate that bioactive glass materials are very interesting options for tissue regeneration and tissue engineering. A sol–gel process produces small bioactive glass particles with a high specific surface area. Such particles thus have potentially higher bioactivity and increased absorption rates [4]. The ionic products from their dissolution (Si and Ca) have the potential to control the cell cycle of the osteoblast progenitor cells and stimulate the genes in bone cells to differentiate enhancing bone regeneration [6]. In addition, Hench and Polak [7] have pointed out that the third-generation biomaterials must be both bioactive and resorbent, and designed to stimulate specific cellular responses at the molecular level. The CaO–SiO_2 system

* Corresponding author at: Biomaterials Group, Materials Engineering Department, Isfahan University of Technology, Isfahan 84156-83111, Iran. Tel.: +98 913 326 6632; fax: +98 311 391 2751.
E-mail address: Alidm14@ma.iut.ac.ir (A. Doostmohammadi).

0272-8842/$36.00 © 2011 Elsevier Ltd and Techna Group S.r.l. All rights reserved.
doi:10.1016/j.ceramint.2011.03.026

Table 1
The relation between zeta potential and stability of particles [9].

Zeta potential [mV]	Stability behavior of the particle
0 to ±5	Rapid coagulation or flocculation
±10 to ±30	Incipient instability
±30 to ±40	Moderate stability
±40 to ±60	Good stability
More than ±61	Excellent stability

is the basis for many of the third-generation tissue regeneration materials presently in development [1].

For particle suspensions in water, zeta potential is the electrical potential difference between the dispersion medium and the stationary layer of fluid attached to the dispersed particle. A value of 25 mV (positive or negative) can be taken as the arbitrary value that separates low-charge surfaces from high-charge surfaces. The significance of zeta potential is that it can be related to the stability of particle dispersions. The zeta potential indicates the degree of repulsion between adjacent, similarly charged particles. For molecules and particles that are small enough, a high zeta potential (negative or positive) will confer stability, i.e. the particles will resist aggregation. When the potential is low, attraction exceeds repulsion and the particles tend to aggregate. So, particles with high zeta potential (negative or positive) are electrically stabilized while particles with low zeta potentials tend to coagulate or flocculate as outlined in Table 1 [8,9].

Also it has been suggested that negative values of zeta potential have a significant favorable effect on the attachment and proliferation of bone cells [10]. Therefore, in addition to zeta potential's effect on particles' behavior in aqueous environments, it also affects the cell behavior around the particles. There are various published reports on the zeta potential of synthetic bioceramics like hydroxyapatite and other calcium phosphates [10–12]. However, it would be necessary to investigate the surface charge of bioactive glass particles with different compositions.

In this study, there is first a description of how the bioactive glass nanoparticles were prepared. Then, methods and results of characterizing the particles in various ways are presented. Characterization included chemical composition, particle morphology, particle size distribution and surface area. In addition the zeta potential of the prepared bioactive glass particles was determined.

2. Materials and methods

2.1. Glass synthesis

Colloidal solutions of 63S composition (63 mol% SiO_2, 28 mol% CaO, 9 mol% P_2O_5) were prepared by mixing deionized water, 2 N hydrochloric acid, tetraethyl orthosilicate (TEOS), triethyl phosphate (TEP) and calcium nitrate [3]. The initial procedure involved mixing TEOS (28.5 ml) and ethanol (40 ml) as an alcoholic media. Deionized water was added to solution and allowed to mix until the solution became clear. The H_2O:(TEOS) molar ratio was 4:1. After 30 min, TEP (2.35 ml) added to the stirring solution. After another 30 min, calcium nitrate (12.1 g) was added. The solution was then stirred for an additional hour. The gel was heated (80 °C, 10 h), dried (140 °C, 15 h) and thermally stabilized (650 °C, 2 h) according to established procedures [13]. The produced glass was ground with a mortar and pestle to disagglomerate the particles. Finally the particles were sieved to make a distribution of particles of size less than 5 μm (L3-M5 5 μm stainless steel sieve & Sonic Sifter Separator, Advantech Manufacturing Co., New Berlin, WI, USA). Bioactive glass particles were sterilized at 180 °C for 1 h.

2.2. Characterization

2.2.1. Elemental composition analysis

The elemental composition of bioactive glass particles was confirmed by X-ray fluorescence spectroscopy (XRF) (PW2404, PHILIPS) and energy dispersive X-ray analysis (EDX) technique (SUPRA 40 VP FE-SEM).

2.2.2. Phase analysis by X-ray diffraction (XRD)

X-ray diffraction (XRD) technique (Philips X'Pert-MPD system with a Cu Kα wavelength of 1.5418 Å) was used to analyze the structure of the prepared bioactive glass. The diffractometer was operated at 40 kV and 30 mA at a 2θ range of 10–90° employing a step size of 0.05°/s.

2.2.3. Particle morphology by scanning electron microscopy (SEM)

Particle samples were mounted on aluminum SEM pins and coated with Au/Pd. They were then observed with a scanning electron microscope (SUPRA 40 VP FE-SEM, Carl Zeiss AG, Germany) operated at an acceleration voltage of 20 kV. The size range of the particles was determined by measuring a statistically relevant numbers of particles from the electron micrographs, using the measuring tools provided for this purpose by Zeiss with their SEM.

2.2.4. In vitro apatite forming ability

The bioactive glass particles, before and after immersion in SBF (simulated body fluid) were examined by Fourier transform infrared spectroscopy (FTIR) with Bomem MB 100 spectrometer (Bruker, Billerica, MA, USA). The particles were immersed in SBF for 30 days at 37 °C then removed from the SBF solution, rinsed using de-ionized water and dried at 90 °C. The composition of SBF, described by Kokubo [14], has an ionic composition similar to that of human blood plasma. SBF is reported to produce the same type of hydroxyapatite layers in vitro, as would form on the glass surface in vivo [3,14]. Transmission IR spectra were recorded under nitrogen atmosphere from 4000 to 100 cm^{-1} with a resolution of 4 cm^{-1}.

2.2.5. Surface area and theoretical particle size by the gas adsorption (BET method)

The specific surface area of bioactive glass samples was measured by determining the N_2-gas adsorption–desorption

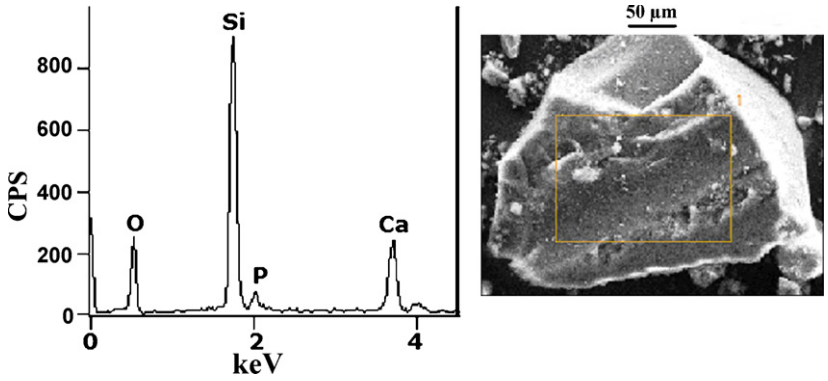

Fig. 1. Left panel: energy dispersive X-ray analysis (EDX) of the bioactive glass particles. The peaks of O, Si, P and Ca indicate the consisting elements of prepared bioactive glass. Right panel: SEM micrograph of one representative particle analyzed.

isotherms using a Brunauer–Emmett–Teller (BET) apparatus (Gemini V analyzer, Micromeritics GmbH, Germany). The samples were degassed at 200 °C under reduced pressure (10–3 Torr) for 16–20 h before each measurement. The amount of nitrogen adsorbed at −196 °C was measured volumetrically.

A theoretical particle size can be calculated from these adsorption data by assuming that the measured surface area for a unit mass of particles is that of a collection of spherical particles of identical size. It can be shown that the resulting theoretical particle diameter, D (in μm), is given by:

$$D = \frac{6}{S_{sp}\rho_a} \quad (1)$$

where S_{sp} is the specific surface area per unit mass of the sample and ρ_a is the theoretical density of the solid material.

2.2.6. Particle size and size distribution by laser dynamic light scattering (DLS)

Particle size and size distribution (dispersity) were assessed with a laser dynamic light scattering (DLS) instrument (Zetasizer-nano series, Malvern Instruments Ltd, Malvern, Worcestershire, UK). This instrument employs a 173° backscatter detector and an N5 submicron particle size analyzer (Beckman–Coulter) using multi-angle measurements (30.1°, 62.6° and 90°). Particle size measuring was done in physiological saline at 37 °C.

2.2.7. Particle dispersion stability by zeta potential measurement

To indicate the stability of particle suspensions, the zeta potential of the particles was measured with a laser Doppler electrophoresis (LDE) instrument (Nano Series, Malvern Instrument Ltd., UK). To roughly simulate in vivo ionic environments, bioactive glass samples were suspended in physiological saline (0.154 M NaCl solution) at pH 5, 7.4, and 9. The suitability of such in vitro studies was addressed by Bagambisa et al. [15], who found that an aqueous in vitro model yielded complementary results when compared to the in vivo results because of the ubiquitous presence of water.

The potential was determined six times (each measurement being the average of 40 runs) and the mean values and standard deviations were calculated. The instrument automatically calculates electrophoretic mobility (U), and zeta potential according to Smoluchowski's equation [16]:

$$\zeta = \frac{U\eta}{\varepsilon} \quad (2)$$

where ζ is the zeta potential, U the electrophoretic mobility, η the medium viscosity and ε is the dielectric constant.

3. Results

3.1. Elemental composition analysis

The result of EDX microanalysis of the glass particles is shown in Fig. 1. The peaks of O, Si, P and Ca indicate the consisting elements of prepared bioactive glass particles.

The existent elements in prepared bioactive glass particles and estimated composition measured by X-ray fluorescence (XRF), is shown in Table 2. The molar percentage of oxides was expressed by computer according to the elemental analysis and considering the assumption that all the elements are in oxidic form.

3.2. X-ray diffraction analysis

The XRD pattern of the prepared glass after heating at 600 °C for 2 h did not contain diffraction maxima, indicative of the internal disorder and the glassy nature of this material (Fig. 2). The XRD pattern of the initial sample confirms its amorphous nature, characterized by the broad diffraction bands.

3.3. Scanning electron microscope

Fig. 3 shows SEM images of the bioactive glass particles. Heterogeneous surfaces consisting of random-sized particles

Table 2
Bioactive glass estimated oxidic composition measured by X-ray fluorescence (XRF).

Oxide	Molar percentage
SiO_2	63.27
CaO	28.47
P_2O_5	9.25

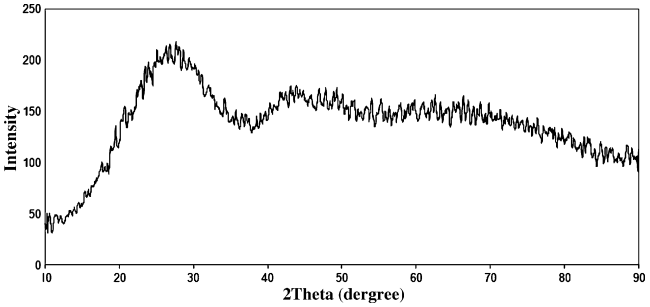

Fig. 2. XRD pattern of the prepared bioactive glass nanoparticles: intensity of diffraction vs. angle of radiation (2θ,°). No peak of diffraction could be observed.

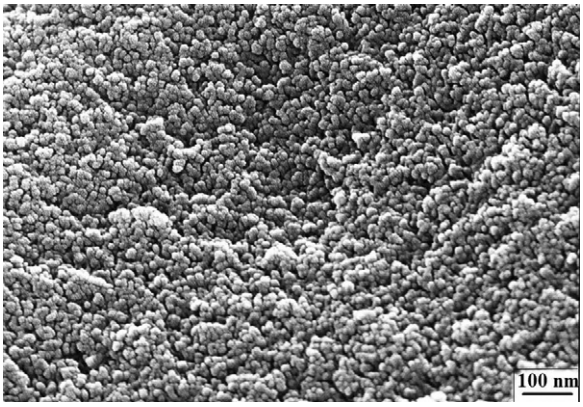

Fig. 3. SEM micrographs of the bioactive glass nanoparticles.

can be seen. SEM confirmed particles are in the nanoscale range (<40 nm) but showed the particles were agglomerated.

3.4. Apatite forming ability

Fourier transform infrared (FTIR) spectra of unreacted 63S bioactive glass and of 63S glass particles after immersion in SBF for 30 days are shown in Fig. 4. The absorption bands had been defined according to the literature [17].

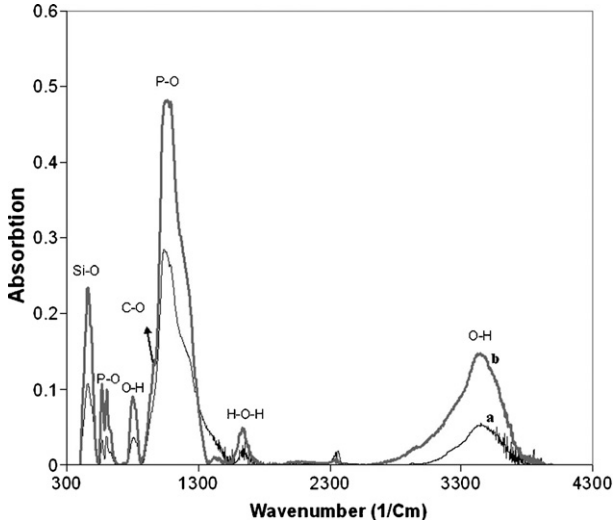

Fig. 4. FTIR spectra of the bioactive glass particles: (a) before soaking in SBF; (b) after 30 days soaking in SBF.

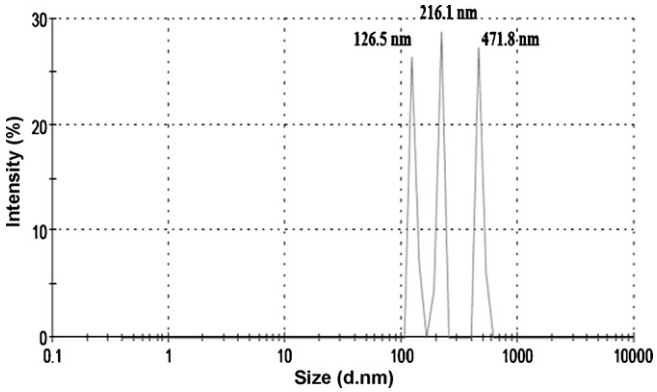

Fig. 5. Average size and size distribution of bioactive glass particles.

3.5. Surface area and theoretical particle size by gas adsorption (BET method)

The BET specific surface area of bioactive glass particles was 223.6 ± 0.5 m^2/g. As explained in Section 2, a theoretical particle size can be calculated from these data using Eq. (2). The calculated theoretical density (ρ_a) of the particles was 1.08 g/cm^3. The resulting theoretical particle size of the bioactive glass particles was ca. 25 nm.

3.6. Particle size and size distribution by laser dynamic light scattering (DLS)

The bioactive glass particle size and size distribution measured by DLS in physiological saline are shown in Fig. 5. As could be seen, the particles range from around 126 to 470 nm in physiological saline. Nearly 30% of particles have an average diameter of 126.5 nm, 40% of them have an average diameter of 216.1 nm and 30% of them have an average of 471.8 nm. The results showed that these particles are relatively agglomerated in physiological saline.

3.7. Zeta potential

The zeta potential of these bioactive glass particles was investigated in physiological saline. The zeta potential of the particles ranged from −7.45 ± 0.74 mV at pH 5 to −16.18 ± 1.8 mV at a typical physiologic pH of 7.4. At pH 9 the zeta potential was −14.31 ± 1.4 mV. In summary, as shown in Fig. 6, the zeta potential varied with pH and was negative at acidic, neutral and basic pH values.

4. Discussion

The EDX results (Fig. 1) indicated that the three main elements in bioactive glass particles (as expected) are Si, Ca and P. XRF analysis showed that the particles are composed of Si, Ca and P oxides. The molar percentages of these elements approximately conforms the molar percentages of their oxides in prepared bioactive glass. These results showed that the composition of prepared bioactive glass is in good agreement with documented composition for sol–gel 63S bioactive glass

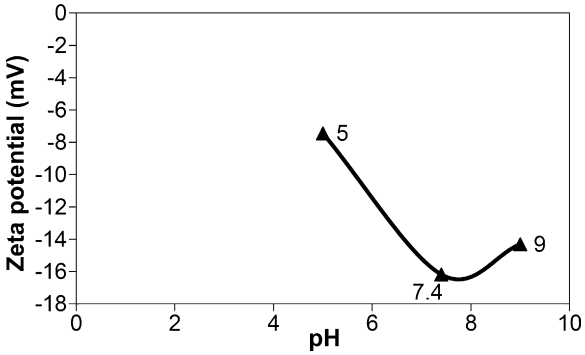

Fig. 6. Zeta potential at three different pH values for 63S bioactive glass particles in physiological saline at 37 °C.

[1]. The XRD patterns were characterized by broad diffraction bands, indicating that the obtained bioactive glass particles were amorphous (Fig. 2), and thus that the sol–gel method could prepare a predominantly glassy material. This is completely in agreement with previous reports [3,18]. According to SEM images (Fig. 3), the prepared bioactive glass particles were less than 40 nm.

As could be seen in FTIR results (Fig. 4), the double peaks of the crystalline P–O vibration mode at 605 and 572 cm^{-1} indicated that the layer of apatite forms on the bioactive glass particles [19]. The absence of 875 and 1418 cm^{-1} bands, that correspond to C–O bending vibrations from CO_3^{2-}, indicated that the apatite formed on the glass particles was hydroxyapatite (HA), not hydroxycarbonateapatite (HCA). This is in agreement with other researchers' results [20]. After 30 days of soaking time, the bands were sharper and their intensities were stronger, indicating high crystallinity of the apatite [3,20].

The surface area of the bioactive glass particles, measured by the BET method, was 223.6 ± 0.5 m^2/g. This value proves that the main particles are really fine, and thus potentially providing (per unit mass of particles) more sites for osteoblast adhesion and osseous formation in bone defects [2,3]. Due to this surface area, sol–gel bioactive glasses also have the potential to resorb much faster than e.g. 45S5 melt-derived bioactive glass with an 0.02 m^2/g surface area, while maintaining the unique bioactive characteristics of the particle [21]. The theoretical particle size calculated from this surface area (Eq. (2)) was ca. 24 nm. The calculation does not mean that the particles are really all around 24 nanometers in diameter but it certainly does confirm that the micron or nano-range agglomerates that form in a solution due to the low zeta potential are comprised of particles in the nanometer range.

There is generally an inverse relationship between size and zeta potential of the nanoparticles [22]. As shown in Fig. 5, the size distribution of the bioactive glass particles ranged from about 100 to 500 nm. SEM and BET measurements indicated that the real size of the particles was less than 40 nm. This difference is related to the particles' zeta potential. Due to the relatively low zeta potential of the particles in physiological saline, the particles become agglomerated and form clusters. However, the size of these clusters was less than 500 nm in physiological saline.

Table 3
Reported zeta potential for bioceramics and bone cells [16].

Sample	Zeta potential in physiological saline
HA (sintered)	$+4.1 \pm 0.9$
HA (unsintered)	$+15 \pm 1.2$
Beta TCP	$+2.4 \pm 0.5$
Osteoblast cells	-40 ± 5
Bone	-70

It has been shown that a negative zeta potential has important biological effects in vivo [11], and low zeta potential promotes cell attachment and proliferation [10,12]. The surface of the particles produced in this study will be charged negatively in expected aqueous biological environments (see Fig. 6). A number of studies have shown that a material that has an electronegative surface charge (negative zeta potential) is more accessible for the attachment and proliferation of osteoblasts than surfaces with no or even positive electric charge [12].

Table 3 shows the reported zeta potential for some conventional bioceramics (in physiological saline), osteoblast cells and bone [16]. As can be seen, hydroxyapatite (HA sintered and unsintered) and beta-tricalcium phosphate (βTCP) have a positive zeta potential—unlike the bioactive glass nanoparticles produced in the present study. Since the favorable effect of negative zeta potential on attachment and proliferation of bone cells has been demonstrated [10–12], some investigators have tried to reduce the positive zeta potential of synthetic HA particles by electrical polarization treatment [12].

The results reported here (Fig. 6) show that at acidic, neutral and basic pH values, the zeta potential of produced 63S bioactive glass particles was negative in physiological saline though not highly so. However, it is of interest that the particles were most negative (less likely to agglomerate) around pH 7.4—typical of the extracellular environment in the musculoskeletal system. The source of the negative potential for 63S bioactive glass found in this study can be related to the chemical composition of glass, particle size and the surrounded environment. However, it could be the subject of future investigations.

5. Conclusions

63S bioactive glass nanoparticles (<40 nm) can be produced through sol–gel method. These particles formed an apatite surface layer over time in SBF. The small particle size (high surface area) and apatite surface layer suggest that a given mass of these particles will release Ca and P ions faster and be absorbed faster than the same mass of larger bioactive glass particles. This may be an advantage in some implant coating and tissue engineering applications. The particles had a rather low negative zeta potential in physiological saline solution, and this may explain their tendency to form 100–500 nm aggregates. However, the negativity was greatest (and thus less likely to induce aggregation) around pH 7.4, typical of the musculoskeletal extracellular environment. Most importantly,

according to the literature, this negative surface potential will make these particles more accessible for the attachment and proliferation of osteoblasts.

The source of negative zeta potential was not determined for bioactive glass nanoparticles produced and evaluated in this study. However, it seems likely that it is due to the particle surface structure and the selected chemical composition (63S). In addition to the use in the present applications of bioactive glasses, particles of this kind—i.e. high surface area, surface-coated with apatite and having a negative zeta potential—might also prove useful as a carrier for antibiotics, genes and growth factors that enhance the healing of bone.

Acknowledgments

Hardy & Otto Frey-Zünd Foundation, Basel CH, Professor A.U. Daniels and Professor U. Pieles (FHNW, Muttenz) for superb technical assistance.

References

[1] L.L. Hench, The story of bioglass, J. Mater. Sci. Mater. Med. 17 (2006) 967–978.
[2] H.J. Brekke, M.J. Toth, Principles of tissue engineering applied to programmable osteogenesis, J. Biomed. Mater. Res. 43 (1998) 380–398.
[3] M.H. Fathi, A. Doostmohammadi, Preparation and characterization of sol–gel bioactive glass coating for improvement of biocompatibility of human body implant, Mater. Sci. Eng. A 474 (2008) 128–133.
[4] P. Sepulveda, J.R. Jones, L.L. Hench, In vitro dissolution of melt-derived 45S5 and sol–gel derived 58S bioactive glasses, J. Biomed. Mater. Res. 61 (2002) 301–311.
[5] I.D. Xynos, M.V.J. Hukkanen, J.J. Batten, L.D. Buttery, L.L. Hench, J.M. Polak, Bioglass 45S5 stimulates osteoblast turnover and enhances bone formation in vitro: implications and applications for bone tissue engineering, Calcif. Tissue Int. 67 (2000) 321–329.
[6] I.D. Xynos, A.J. Edgar, L.D.K. Buttery, L.L. Hench, J.M. Polak, Gene-expression profiling of human osteoblasts following treatment with the ionic products of bioglass 45S5 dissolution, J. Biomed. Mater. Res. 55 (2001) 151–157.
[7] L.L. Hench, J.M. Polak, Third-generation biomedical materials, Science 295 (2002) 1014–1022.
[8] N. Schultz, G. Metreveli, M. Franzreb, F.H. Frimmel, C. Syldatk, Zeta potential measurement as a diagnostic tool in enzyme immobilization, Colloids Surf. B: Biointerfaces 66 (2008) 39–44.
[9] Zeta Potential of Colloids in Water and Waste Water, ASTM Standard D 4187-82, American Society for Testing and Materials, 1985.
[10] J.J. Cooper, J.A. Hunt, The significance of zeta potential in osteogenesis, in: Transactions of the 31st Annual Meeting for Biomaterials, Society for Biomaterials, (2006), p. 592.
[11] R. Smeets, A. Kolk, M. Gerressen, O. Driemel, O. Maciejewski, B. Hermanns-Sachweh, D. Riediger, J.M. Stein, A new biphasic osteoinductive calcium composite material with a negative zeta potential for bone augmentation, Head Face Med. 5 (2009) 13.
[12] N.C. Teng, S. Nakamura, Y. Takagi, Y. Yamashita, M. Ohgaki, K. Yamashita, A new approach to enhancement of bone formation by electrically polarized hydroxyapatite, J. Dent. Res. 80 (2001) 1925–1929.
[13] J.E. Gougha, J.R. Jonesb, L.L. Hench, Nodule formation and mineralization of human primary osteoblasts cultured on a porous bioactive glass scaffold, Biomaterials 25 (2004) 2039–2046.
[14] T. Kokubo, H. Takadama, How useful is SBF in predicting in vivo bone bioactivity? Biomaterials 27 (2006) 2907–2915.
[15] F.B. Bagambisa, U. Joos, W. Schilli, Mechanisms and structure of the bond between bone and hydroxyapatite, J. Biomed. Mater. Res. 27 (1993) 1047–1055.
[16] D.A. Oppermann, M.J. Crimp, D.M. Bement, In vitro stability predictions for the bone/hydroxyapatite composite system, J. Biomed. Mater. Res. 42 (1998) 412–416.
[17] M.R. Filgueiras, G.P. LaTorre, L.L. Hench, Solution effects on the surface reactions of three bioactive glass compositions, J. Biomed. Mater. Res. 27 (1993) 1485–1493.
[18] A. Balamurugan, G. Balossier, S. Kannan, J. Michel, A.H.S. Rebelo, J.M.F. Ferreira, Development and in vitro characterization of sol–gel derived $CaO–P_2O_5–SiO_2–ZnO$ bioglass, Acta Biomater. 3 (2007) 255–262.
[19] X. Chen, Y. Meng, Y. Li, N. Zhao, Investigation on bio-mineralization of melt and sol–gel derived bioactive glasses, Appl. Surf. Sci. 255 (2008) 562–564.
[20] D.L. Wheeler, E.J. Eschbach, R.G. Hoellrich, T.J. Montfort, D.L. Chamberland, Assessment of resorbable bioactive material for grafting of critical-size cancellous defects, J. Orthop. Res. 18 (2000) 140–148.
[21] K. Cheng, W. Weng, H. Wang, S. Zhang, In vitro behavior of osteoblast-like cells on fluoridated hydroxyapatite coatings, Biomaterials 26 (2005) 6288–6295.
[22] I.O. Smith, M.J. Baumann, L.R. McCabe, Electrostatic interactions as a predictor for osteoblast attachment to biomaterials, J. Biomed. Mater. Res. A 70 (2004) 436–441.